Prediction of Total Pressure Drop in Stenotic Coronary Arteries with Their Geometric Parameters

Jaerim Kim[*], Dohyun Jin[*], Haecheon Choi[*], Jihoon Kweon[**], Young-Hak Kim[**], Dong Hyun Yang[**] and Namkug Kim[**]
Corresponding author: choi@snu.ac.kr

* Department of Mechanical and Aerospace Engineering, Seoul National University, Seoul, Korea.
** Department of Cardiology, University of Ulsan College of Medicine, Asan Medical Center, Seoul, Korea.

Abstract: It is essential to accurately assess the severity of a coronary artery stenosis. However, assessments based on the extent of diameter or area reduction (DS or AS) is known to over- or underestimate the functional severity of stenosis, pressure drop. Therefore, we investigate the effects of other geometric characteristics as well as AS on the total pressure drop. The numerical simulations of 31 patient-specific coronary arteries and 4 idealized stenosis models are conducted. In the converging part of the stenosis, the skewed velocity profiles toward the outer wall and secondary flow structures in a curved section are observed. Based on them, the total pressure drop in the converging part is estimated from the classical viscous theory assuming the vessel as a series of curved pipes. The total pressure drop in the diverging part is estimated by machine learning technique using geometric parameters suggested in this study. The prediction of total pressure drop is more accurate when we consider the curvature, length, and posterior structure of a stenosis in addition to the minimum diameter or area.

Keywords: Total Pressure Drop, Coronary Artery Stenosis, Curvature, Viscous Theory, Machine Learning.

1   Introduction

Coronary arteries play an important role in supplying blood to the heart, so that stenosis within them may cause serious heart failures, and even death. Therefore, it is important to determine the severity of coronary artery stenosis. There are two methods to diagnose the risk of coronary artery stenosis; an assessment of the degree of reduction in diameter (DS) or area (AS) of a stenosis from coronary angiography, and an assessment of the pressure drop across a stenosis by inserting a pressure wire into the stenosed vessel. In clinical practice, it has been commonly used to measure DS or AS from angiography, instead of pressure drop, due to the lower price or relatively convenient procedure. However, some studies have shown that these geometric-based diagnostics are not highly correlated with the pressure drop which represents the actual severity of a stenosis [1]. Therefore, a number of studies have been performed to investigate the effects of other geometric factors on the pressure drop caused by stenosis [2, 3, 4]. Also, several studies have been carried out to predict the pressure drop based on the geometric characteristics of a stenosis [5, 6, 7]. Although Young & Tsai [5] proposed an equation for the pressure drop approximation for the idealized axisymmetric and nonsymmetric stenosis models, the empirical coefficients should be determined a posteriori by regression for each model.

Schrauwen et al. [6, 7] estimated the pressure drop in stenotic coronary arteries based on their patient-specific geometries. In [6], each artery was deconstructed into four models, adding complexity; straight, tapered, stenosed, and curved models. From the simulation results, they found the relations between additional pressure drops and geometries, but the simulations were conducted in limited geometries such as mildly diseased arteries. In [7], they estimated the pressure drop in straightened stenotic coronary arteries by substituting the predicted velocity profile with geometric parameters into simplified Navier-Stokes equations. However, it cannot be applied to real vessels having curvatures. Therefore, in the present study, we use 31 patient-specific coronary artery models reconstructed from CT images and 4 idealized stenosis models of [8]. Direct numerical simulations are performed to identify the geometric parameters that affect the pressure drop. On the basis of them, we propose a method to predict total pressure drop using fluid mechanics and machine learning for various shapes of patient-specific coronary artery stenoses.

2   Numerical details

Figure 1 shows the schematic diagram of the computational domain. Simulations are conducted at the Reynolds numbers of 100, 200, and 300 based on the area and flow rate of the reference vessel (see Figure 1). The governing equations for blood flow are the continuity and incompressible Navier-Stokes equations:

$$\frac{\partial u_i}{\partial x_i} = 0, \tag{1}$$

$$\rho \left(\frac{\partial u_i}{\partial t} + \frac{\partial u_i u_j}{\partial x_j} \right) = -\frac{\partial p}{\partial x_j} + \mu \frac{\partial^2 u_i}{\partial x_j \partial x_j}. \tag{2}$$

An unstructured finite volume method is used to solve the governing equations [9]. We apply the second-order time-accurate fractional step method [10] and symmetric interpolation for arbitrarily non-uniform meshes [11] for the time advancement and spatial discretization, respectively. A constant flow rate with uniform velocity profile is used at the inlet, and a resistance boundary condition [12] is applied for each coronary outlet.
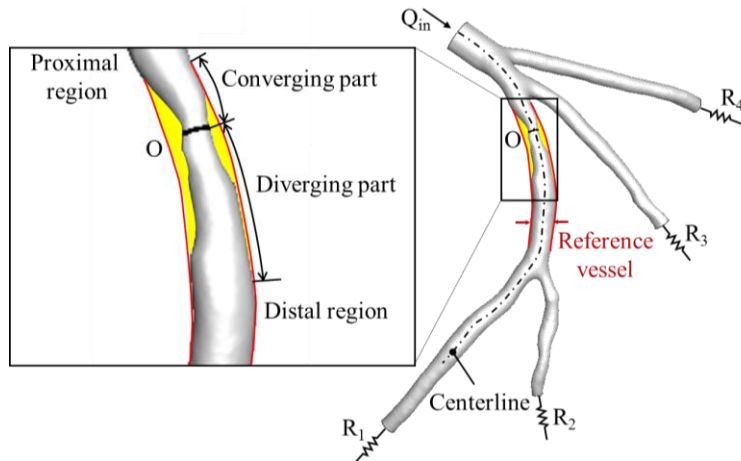

Figure 1: Computational domain of a coronary artery model. The point O indicates the position where the cross-sectional area of a stenosis becomes the minimum.

3 Result and discussion

3.1 Total pressure drops in stenotic coronary arteries

Figure 2 (a) shows the nondimensional total pressure drop versus the AS for 31 patient-specific and 4 idealized stenosis models at Re = 200. It is noticeable that, even with a similar AS, different models have similar (e.g., P13 and P29) or significantly different (e.g., P13 and P5) nondimensional total pressure drops. Also, some models such as P13 and P29 have total pressure drops similar to those of models having much larger AS. Figures 2 (b) and (c) show the nondimensional total pressure drops in the converging and diverging parts, respectively. The nondimensional total pressure drops in the converging part are smaller than those in the diverging part for most models (see the y-axis scale differences in these figures). The nondimensional total pressure drop in the converging part has less relevance to the AS, while that in the diverging part shows a rather strong relationship with the AS. However, even with similar AS's, considerable differences in the total pressure drop are observed among various models (Figure 2 (c)). Therefore, there is an additional total pressure drop due to structural differences among models in the diverging part.
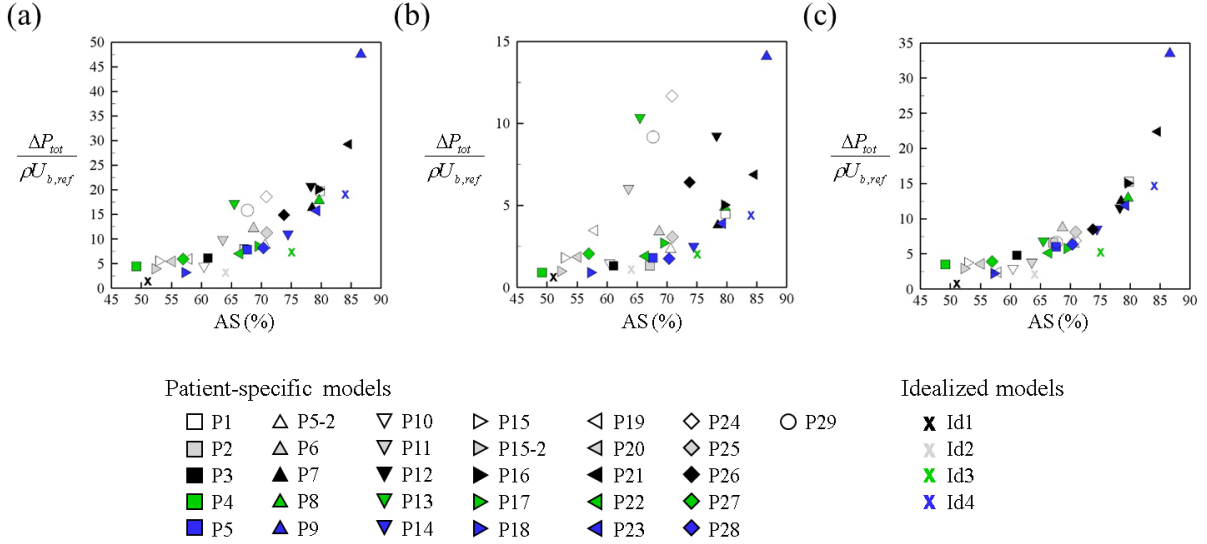

Figure 2: Nondimensional total pressure drops in the (a) whole, (b) converging, and (c) diverging parts of the stenosis.

3.2 Prediction of the total pressure drop in the converging part of stenosis

The P29 has a high nondimensional total pressure drop in the converging part of a stenosis among models having similar AS. The contours of normalized streamwise velocity and total pressure variation along the centerline of the vessel are shown in Figure 3. In the converging part, we observe apparent curvatures of vessel centerline and skewed velocity distribution toward the outer wall. We predict the total pressure drop in the converging part with the classical viscous theory by assuming the blood vessel as a series of curved pipes [13]. We also consider the vessel as a series of straight pipes and apply the viscous theory to predict the total pressure distribution. As shown in Figure 3 (b), the total pressure along the centerline of the vessel is well predicted by the viscous theory with curved pipe assumption, whereas it is not accurately predicted with straight pipe approaximation. This indicates that not only AS but also length and curvature of a stenosis have significant effects on total pressure drop. On the other hand, this simple viscous theory cannot predict the total pressure variation in the diverging part due to large reverse flow region there (Figure 3 (a)). Therefore, a separate approach is required to predict the total pressure in the diverging part of a stenosis.
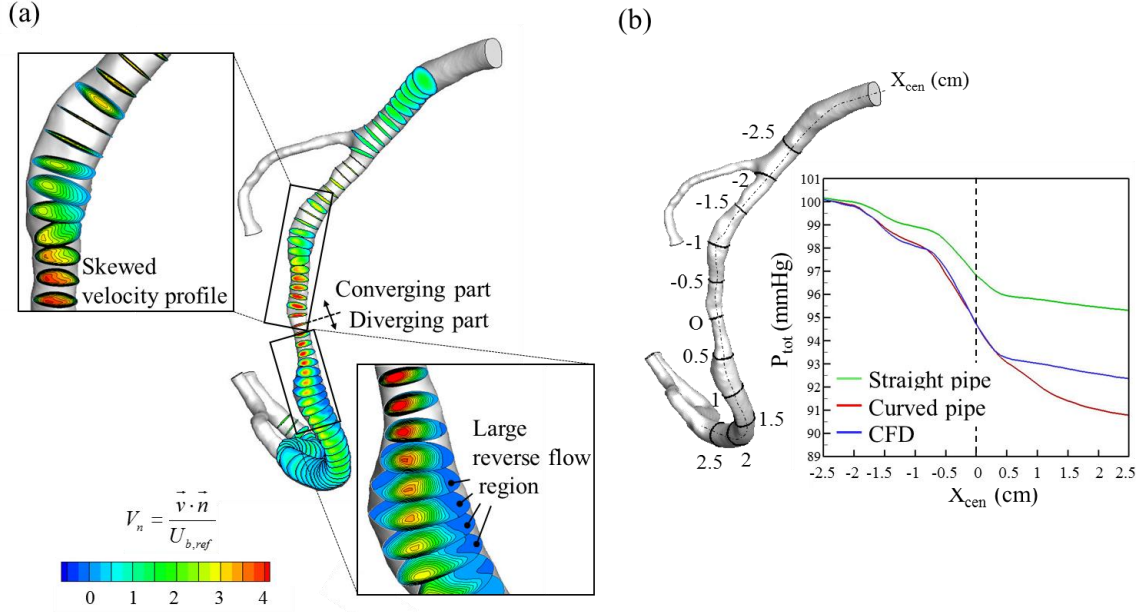
Figure 3: Flow characteristics in the converging part of P29: (a) contours of the streamwise velocity; (b) variation of total pressure along the centerline of the vessel and those predicted with assumptions of straight and curved pipes.

3.3 Prediction of total pressure drops in the diverging part of the stenosis

Figure 4 (a) shows the contours of the normalized streamwise velocity in the diverging parts of P3 and P10. P3 and P10 have similar AS's but very different nondimensional total pressure drops. In the case of P3 where the total pressure loss is rather large, the flow direction is greatly changed in the diverging part, whereas P10 has a rather straight diverging part. Thus, we suggest geometric parameters, θ and l_θ (Figure 4 (b)), and the total pressure drop in the diverging part is estimated using kernel ridge regression (KRR), one of the well-known machine learning techniques, with these geometric parameters. To consider the total pressure drop depending on the flow rate, we consider Re = 100, 200, and 300 for each coronary artery model. The input features include minimum diameter (d_{min}/d_{ref}), $\sin\theta$, l_θ/d_{ref} and Re. The data set is randomly split into training and test set as 7:3 ratio, and the test set is used to validate the machine learning model. Figure 5 shows the comparison of the total pressure drops in the diverging part from CFD and machine learning. Although the pressure drop in the diverging part is dominantly determined by d_{min}/d_{ref} ($R^2 = 0.82$), higher coefficients of determination are obtained when including other parameters: e.g., $R^2 = 0.92, 0.84, 0.85$ in Figures 5 (b), (c) and (d), respectively.
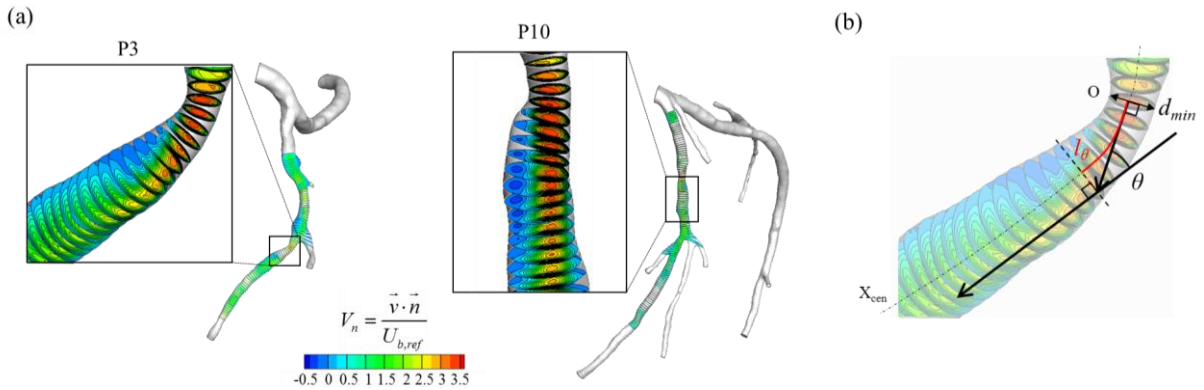

Figure 4: Flow characteristics in the diverging part of P3 and P10, and definitions of geometric parameters: (a) contours of the streamwise velocity; (b) θ and l_θ.
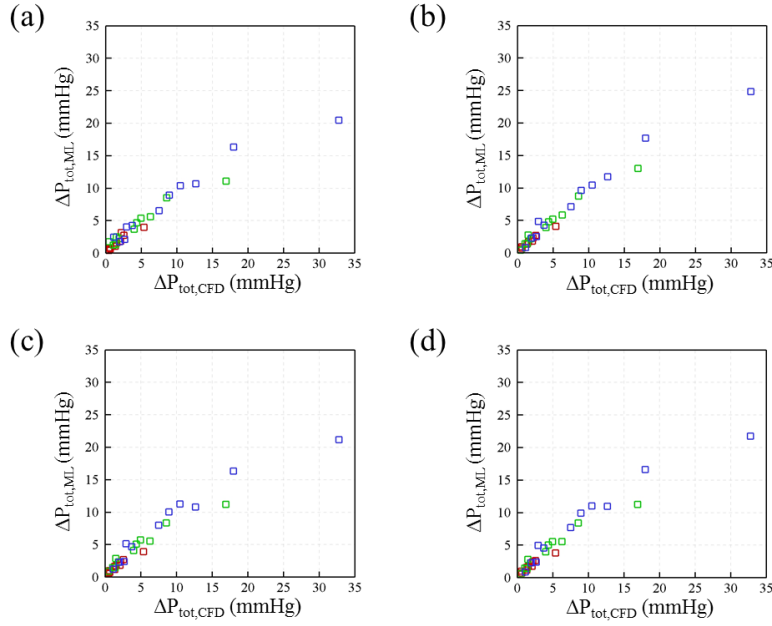
4

Figure 5: Comparisons of the total pressure drop in the diverging part of stenosis from CFD and machine learning: with various input feature combinations: (a) d_{min}/d_{ref} and Re; (b) d_{min}/d_{ref}, l_θ/d_{ref} and Re; (c) d_{min}/d_{ref}, $\sin\theta$ and Re; (d) d_{min}/d_{ref}, l_θ/d_{ref}, $\sin\theta$ and Re. Here, red, green and blue symbols denote the cases of Re = 100, 200 and 300, respectively.

3.4 Prediction of total pressure drops in the stenotic coronary arteries

Figures 6 shows the comparison of the total pressure drops between the CFD results and present predictions in the converging, diverging, and whole parts, respectively. In Figure 6, the results from CFD and prediction are well correlated when considering curvature, l_θ/d_{ref} and d_{min}/d_{ref} ($R^2 = 0.95$) than only considering d_{min}/d_{ref} ($R^2 = 0.82$).
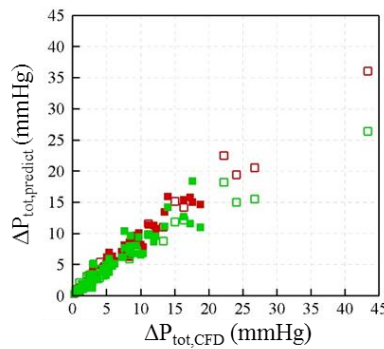

Figure 6: Comparisons of the total pressure drop from CFD and present prediction. Here, the red symbols are the prediction considering l_θ/d_{ref} and d_{min}/d_{ref}, and green symbols are the prediction considering only d_{min}/d_{ref}. solid and open symbols represent the training and test sets.

4   Conclusions

We introduced a classical viscous theory assuming the converging part of a stenosis as a curved-connected pipe and machine learning method in the diverging part of the stenosis, to predict the total pressure drop. 31 patient-specific and 4 idealized models were used in this study. The total pressure drop across the stenosis was well predicted by the present approach. In the present study, we consider steady inflow only. In the future, pulsatile inflow conditions will be considered.

Acknowledgments

References

[1] S.-J. Park, S.-J. Kang, J.-M. Ahn, E.B. Shim, Y.-T. Kim, S.-C. Yun, H. Song, J.-Y. Lee, W.-J. Kim, D.-W. Park, S. Lee, Y. Kim, C. Lee, G. S. Mintz and S. Park. Visual-functional mismatch between coronary angiography and fractional flow reserve. JACC. Cardiovasc. Interv., 5:1029-1036, 2012.

[2] S. Kamangar, G. Kalimuthu, I. Anjum Badruddin, A. Badarudin, N. Salman Ahmed and T. Khan. Numerical investigation of the effect of stenosis geometry on the coronary diagnostic parameters. Sci. World. J., 2014: 354946, 2014.

[3] K. Govindaraju, G.N. Viswanathan, I.A. Badruddin, S. Kamangar, N. Salman Ahmed and A.A. Al-Rashed. The influence of artery wall curvature on the anatomical assessment of stenosis severity derived from fractional flow reserve: a computational fluid dynamics study. Comput. Methods. Biomech. Biomed. Eng., 19:1541-1549, 2016.

[4] C. Peng, X. Wang, Z. Xian, X. Liu, W. Huang, P. Xu and J. Wang. The impact of the geometric characteristics on the hemodynamics in the stenotic coronary artery. PloS one. 11:e0157490, 2016.

[5] D.F. Young and F.Y. Tsai. Flow characteristics in models of arterial stenoses—I. Steady flow. J. Biomech. 6:395-402, 1973.

[6] J. Schrauwen, J. Wentzel, A. van der Steen and F. Gijsen. Geometry-based pressure drop prediction in mildly diseased human coronary arteries. J. Biomech., 47:1810-1815, 2014.

[7] J.T. Schrauwen, D.J. Koeze, J.J. Wentzel, F.N. van de Vosse, A.F. van der Steen and F.J. Gijsen. Fast and accurate pressure-drop prediction in straightened atherosclerotic coronary arteries. Ann. Biomed. Eng., 43:59-67, 2015.

[8] S.S. Varghese, S.H. Frankel and P.F. Fischer. Direct numerical simulation of stenotic flows. Part 1. Steady flow. Journal of Fluid Mechanics. 582:253-280, 2007.

[9] D. Kim and H. Choi. A second-order time-accurate finite volume method for unsteady incompressible flow on hybrid unstructured grids. J. Comput. Phys., 162:411-428, 2000.

[10] H. Choi and P. Moin. Effects of the computational time step on numerical solutions of turbulent flow. J. Comput. Phys., 113:1-4, 1994.

[11] K. Mahesh, G. Constantinescu and P. Moin. A numerical method for large-eddy simulation in complex geometries. J. Comput. Phys., 197:215-240, 2004.

[12] I.E. Vignon-Clementel, C.A. Figueroa, K.E. Jansen and C.A. Taylor. Outflow boundary conditions for three-dimensional finite element modeling of blood flow and pressure in arteries. Computer methods in applied mechanics and engineering. 195:3776-3796, 2006.

[13] C. White. Streamline flow through curved pipes. Proc. R. Soc. Lond. A., 123:645-663, 1929.